J|A|C|S
ARTICLES
Published on Web 09/05/2002

Structural Studies of the Carbon Monoxide Complex of [NiFe]hydrogenase from *Desulfovibrio vulgaris* Miyazaki F: Suggestion for the Initial Activation Site for Dihydrogen

Hideaki Ogata,[†] Yasutaka Mizoguchi,[‡] Nobuhiro Mizuno,[†] Kunio Miki,[†,§] Shin-ichi Adachi,[§] Noritake Yasuoka,[||] Tatsuhiko Yagi,[⊥] Osamu Yamauchi,[‡,#] Shun Hirota,*[,‡] and Yoshiki Higuchi*[,†,§,▽]

Contribution from the Division of Chemistry, Graduate School of Science, Kyoto University, Sakyo-ku, Kyoto 606-8502, Japan, Department of Chemistry, Graduate School of Science, Nagoya University, Furo-cho, Chikusa-ku, Nagoya 464-8602, Japan, RIKEN Harima Institute/SPring-8, 1-1-1 Koto, Mikazuki-cho, Sayo-gun, Hyogo 679-5248, Japan, Department of Life Science, Faculty of Science, Himeji Institute of Technology, 3-2-1 Koto, Kamigori-cho, Ako-gun, Hyogo 678-1297, Japan, and Shizuoka University, 836 Oya, Shizuoka 422-8529, Japan

Received December 3, 2001

Abstract: The carbon monoxide complex of [NiFe]hydrogenase from *Desulfovibrio vulgaris* Miyazaki F has been characterized by X-ray crystallography and absorption and resonance Raman spectroscopy. Nine crystal structures of the [NiFe]hydrogenase in the CO-bound and CO-liberated forms were determined at 1.2−1.4 Å resolution. The exogenously added CO was assigned to be bound to the Ni atom at the Ni−Fe active site. The CO was not replaced with H_2 in the dark at 100 K, but was liberated by illumination with a strong white light. The Ni−C distances and Ni−C−O angles were about 1.77 Å and 160°, respectively, except for one case (1.72 Å and 135°), in which an additional electron density peak between the CO and Sγ(Cys546) was recognized. Distinct changes were observed in the electron density distribution of the Ni and Sγ(Cys546) atoms between the CO-bound and CO-liberated structures for all the crystals tested. The novel structural features found near the Ni and Sγ(Cys546) atoms suggest that these two atoms at the Ni−Fe active site play a role during the initial H_2-binding process. Anaerobic addition of CO to dithionite-reduced [NiFe]hydrogenase led to a new absorption band at about 470 nm (∼3000 $M^{-1}cm^{-1}$). Resonance Raman spectra (excitation at 476.5 nm) of the CO complex revealed CO-isotope-sensitive bands at 375/393 and 430 cm^{-1} (368 and 413 cm^{-1} for $^{13}C^{18}O$). The frequencies and relative intensities of the CO-related Raman bands indicated that the exogenous CO is bound to the Ni atom with a bent Ni−C−O structure in solution, in agreement with the refined structure determined by X-ray crystallography.

Introduction

Hydrogenases catalyze the reversible oxidation of molecular hydrogen and play a key role in hydrogen metabolism in various bacteria. Dihydrogen, the substrate and product of hydrogenases, is a good candidate for fuel in the future, since fossil fuels are a limited resource and considered to cause environmental disruption. The reaction mechanism of dihydrogen production by hydrogenases is potentially useful for development of new chemical engineering processes for hydrogen fuels, whereas that of dihydrogen consumption is potentially applicable for new types of fuel cells.

Hydrogenases are classified into several groups according to the metal composition of their active sites. So far, [nonmetal], [Fe], [NiFe], and [NiFeSe] hydrogenases have been identified. Among them, [NiFe]hydrogenases are the most widely investigated.[1−7] The hydrogenase from *Desulfovibrio vulgaris* Miyazaki F is composed of a heterodimer with a total molecular mass of 91 kDa (α = 62.5 kDa and β = 28.8 kDa). The active site of the [NiFe] hydrogenases in the oxidized form is composed of the Ni and Fe atoms with four cysteinyl sulfur and four nonprotein ligands (Figure 1).[8] The nonprotein L1, L2, and L3

* To whom correspondence should be addressed. (Dr. Yoshiki Higuchi) Phone: +81-791-58-0179. FAX: +81-791-58-0177. E-mail: hig@sci.himeji-tech.ac.jp. (Dr. Shun Hirota) Phone: +81-52-789-2952. FAX: +81-52-789-2953. E-mail: k46230a@nucc.cc.nagoya-u.ac.jp.
[†] Kyoto University.
[‡] Nagoya University.
[§] RIKEN Harima Institute/SPring-8.
[||] Himeji Institute for Technology.
[⊥] Shizuoka University
[#] Present address: Unit of Chemistry, Faculty of Engineering, Kansai University, Yamate-cho, Suita, Osaka 564-8680, Japan.
[▽] Department of Life Science, Graduate School of Science, Himeji Institute of Technology, 3-2-1 Koto, Kamigori-cho, Ako-gun, Hyogo 678-1297, Japan.

(1) Adams, M. W. W.; Mortenson, L. E.; Chen, J. S. *Biochim. Biophys. Acta* **1980**, *594*, 105−176.
(2) Albracht, S. P. J. *Biochim. Biophys. Acta* **1994**, *1188*, 167−204.
(3) Fontecilla-Camps, J. C. *J. Bio. Inorg. Chem.* **1996**, *1*, 91−98.
(4) Frey, M. *Struct. Bonding* **1998**, *90*, 97−126.
(5) Cammack, R.; van Vliet, P. *Bioinorganic Catalysis*, 2nd ed.; Marcel Dekker: New York, 1999.
(6) Darensbourg, M. Y.; Lyon, E. J.; Smee, J. *J. Coord. Chem. Rev.* **2000**, *206*, 533−561.
(7) Vignais, P. M.; Billoud, B.; Meyer, J. *FEMS Microbiol. Rev.* **2001**, *25*, 455−501.
(8) Higuchi, Y.; Yagi, T.; Yasuoka, N. *Structure* **1997**, *5*, 1671−1680.

10.1021/ja012645k CCC: $22.00

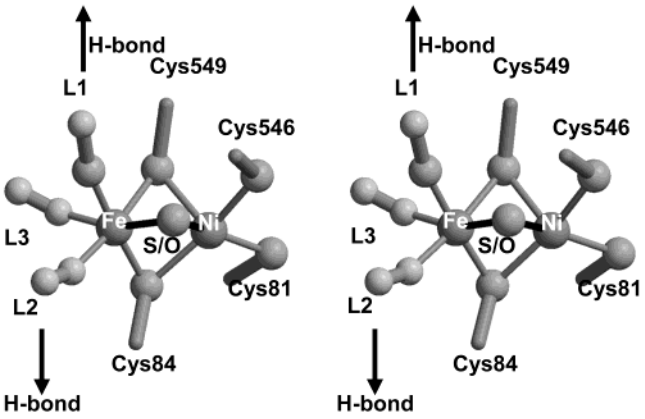

Figure 1. Structure of the Ni−Fe active site of [NiFe]hydrogenase in the oxidized form; L1= SO, CN, or CO; L2= CN or CO; L3 = CN or CO. This figure was prepared using MOLSCRIPT,[9] and Raster3D.[10]

ligands bound to the Fe atom were assigned as SO, CN or CO, CN or CO, and CN or CO molecules, and a bridging ligand between the Ni and Fe atoms as S or SH, as the most probable candidates for the enzyme from *D. v.* Miyazaki. A CN or CO molecule, however, was also possible instead of the SO.[8] In contrast, CO, CN, CN, and O or OH ligands were assigned in the respective ligand positions for the *D. gigas* enzyme.[11,12] The two diatomic ligands of L1 and L2 in Figure 1 are hydrogen-bonded to the side-chain atoms of Arg479 (Arg463 in *D. gigas* enzyme) and Ser502 (Ser486 in *D. gigas* enzyme), respectively. The bridging S or SH ligand between the Ni and Fe atoms in *D. v.* Miyazaki enzyme is liberated from the active site during the reductive activation process of the enzyme under the atmosphere of H_2.[13,14] Likewise, the bridging O/OH ligand in *D. gigas* enzyme is liberated during the reductive activation of the enzyme.[15]

Carbon monoxide (CO) was known as a reversible inhibitor of hydrogenases in earlier enzymatic studies.[16−20] The H_2 evolution activity of the [NiFe]hydrogenase from *D. v.* Miyazaki decreased as the partial pressure of CO was increased, whereas the original activity recovered upon flushing out CO with a stream of N_2.[21] The data from spectroscopic studies have suggested that CO binds to the Ni atom at the active site for [NiFe]hydrogenase from *Chromatium vinosum*.[22−24] Introduction of ^{13}CO caused a 2-fold superhyperfine splitting of its Ni EPR spectrum, which demonstrates that one CO molecule directly binds to the Ni atom in an axial position.[24] The C−O stretching (ν_{CO}) IR band, which has been detected for the CO complex of the *C. vinosum* [NiFe]hydrogenase, showed that the CO ligand is photolabile at cryogenic temperature but could rebind to restore the original CO complex at temperatures above 200 K.[25] An EPR study also indicated that the CO-bound species appeared only after thawing the CO-photodissociated species under a CO atmosphere.[23] Presteady-state kinetics of the reactions of the *C. vinosum* enzyme with H_2 and CO revealed that the S = 1/2, EPR-detectable state (one electron oxidized from the fully reduced state) was induced from the fully reduced state after 11 ms by replacing H_2 with CO.[26] In addition, a linear coordination mode of an exogenous CO to the Ni atom was suggested by a recent X-ray absorption spectroscopic study on the *C. vinosum* enzyme.[27] The characteristics of the CO-complex of the [Fe]hydrogenase from *Clostridium pasteurianum* have been studied in detail by EPR spectroscopy and X-ray crystallography.[28,29]

While various lines of evidence indicated that the extrinsic CO interacts with the Ni atom of [NiFe]hydrogenase, they were not entirely conclusive, given the heterobinulcear nature of the active site and the intimate communication between the two metals. In this study, we present the first direct evidence of CO coordination to the Ni atom of *D. v.* Miyazaki [NiFe]hydrogenase by X-ray crystallography and optical absorption and resonance Raman spectroscopy. Some novel features of the electron density distribution were observed at the active site of the CO-bound and CO-liberated forms in the crystal structures at 1.20−1.40 Å resolution. The possible initial reaction site for H_2 is also discussed.

Experimental Section

Enzyme Purification. Isolation and purification of the oxidized [NiFe]hydrogenase from *D. v.* Miyazaki F was carried out according to the protocol described previously.[30] A solution of the enzyme was concentrated to about 1 mM using a Centricon-30 filter and stored at 77 K for later use. $^{12}C^{16}O$ (Nippon Sanso, 99.95 atom %, O_2 less than 75 ppm), $^{13}C^{18}O$ (ICON, 99 atom % for ^{13}C and 95 atom % for ^{18}O), and H_2 (Nippon Sanso, 99.9999 atom %, O_2 less than 0.1 ppm) were used.

X-ray Crystallographic Analysis. Crystallization of the oxidized enzyme was achieved by using the sitting-drop vapor diffusion method as described previously.[30] Methyl viologen (final concentration = 1 mM) was added to the protein droplets in order to reduce the crystalline enzyme under the H_2 atmosphere. The crystal space group is $P2_12_12_1$, and the unit cell parameters are shown in Table 1. Diffraction data were collected at 1.20−1.40 Å resolution with the use of Rigaku R-AXIS IV and MAR-CCD detector systems at the SPring-8 beamlines BL-44B2 and BL-41XU (Hyogo, Japan). When the CCD detector was used, diffraction data sets in the low and high-resolution ranges were

(9) Kraulis, P. J. *J. Appl. Crystallogr.* **1991**, *24*, 946−950.
(10) Merrit, E. A.; Murphy, M. E. *Acta Crystallogr.* **1994**, *D50*, 869−873.
(11) Volbeda, A.; Garcin, E.; Piras, C.; de Lacey, A.; Fernandez, V. M.; Hatchikian, E. C.; Frey, M.; Fontecilla-Camp, J. *J. Am. Chem. Soc.* **1996**, *118*, 12969−12996.
(12) Happe, R. P.; Roseboom, W.; Pierik, A. J.; Albracht, S. P. J.; Bagley, K. A. *Nature* **1997**, *385*, 126.
(13) Higuchi, Y.; Ogata, H.; Miki, K.; Yasuoka, N.; Yagi, T. *Struct. Fold Des.* **1999**, *7*, 549−556.
(14) Higuchi, Y.; Yagi, T. *Biochem. Biophys. Res. Commun.* **1999**, *255*, 295−299.
(15) Carepo, M.; Tierney, D. L.; Brondino, C. D.; Yang, T. C.; Pamplona, A.; Telser, J.; Moura, I.; Moura, J. J. G.; Hoffman, B. M. *J. Am. Chem. Soc.* **2002**, *124*, 281−286.
(16) Thauer, R. K.; Kaufer, B.; Zahringer, M.; Jungermann, K. *Eur. J. Biochem.* **1974**, *42*, 447−452.
(17) Yagi, T.; Honya, M.; Tamiya, N. *Biochim. Biophys. Acta* **1968**, *153*, 699−705.
(18) Gruzinskii, I. V.; Gogotov, I. N.; Bechina, E. M.; Semenov Ia, V. *Mikrobiologiia* **1977**, *46*, 625−631.
(19) Daday, A.; Lambert, G. R.; Smith, G. D. *Biochem. J.* **1979**, *177*, 139−144.
(20) Adams, M. W.; Hall, D. O. *Biochem. J.* **1979**, *183*, 11−22.
(21) Yagi, T.; Kimura, K.; Daidoji, H.; Sakai, F.; Tamura, S. *J. Biochem.* **1976**, *79*, 661−671.
(22) Bagley, K. A.; Van Garderen, C. J.; Chen, M.; Duin, E. C.; Albracht, S. P.; Woodruff, W. H. *Biochemistry* **1994**, *33*, 9229−9236.
(23) van der Zwaan, J. W.; Albracht, S. P. J.; Fontijn, R. D.; Roelofs, Y. B. M. *Biochim. Biophys. Acta* **1986**, *872*, 208−215.
(24) van der Zwaan, J. W.; Coremans, J. M.; Bouwens, E. C.; Albracht, S. P. *Biochim. Biophys. Acta* **1990**, *1041*, 101−110.
(25) Bagley, K. A.; Duin, E. C.; Roseboom, W.; Albracht, S. P.; Woodruff, W. H. *Biochemistry* **1995**, *34*, 5527−5535.
(26) Happe, R. P.; Roseboom, W.; Albracht, S. P. J. *Eur. J. Biochem.* **1999**, *259*, 602−608.
(27) Davidson, G.; Choudhury, S. B.; Gu, Z.; Bose, K.; Roseboom, W.; Albracht, S. P.; Maroney, M. J. *Biochemistry* **2000**, *39*, 7468−7479.
(28) Lemon, B. J.; Peters, J. W. *Biochemistry* **1999**, *38*, 12969−12973.
(29) Bennett, B.; Lemon, B. J.; Peters, J. W. *Biochemistry* **2000**, *39*, 7455−7460.
(30) Higuchi, Y.; Yasuoka, N.; Kakudo, M.; Katsube, Y.; Yagi, T.; Inokuchi, H. *J. Biol. Chem.* **1987**, *262*, 2823−2825.

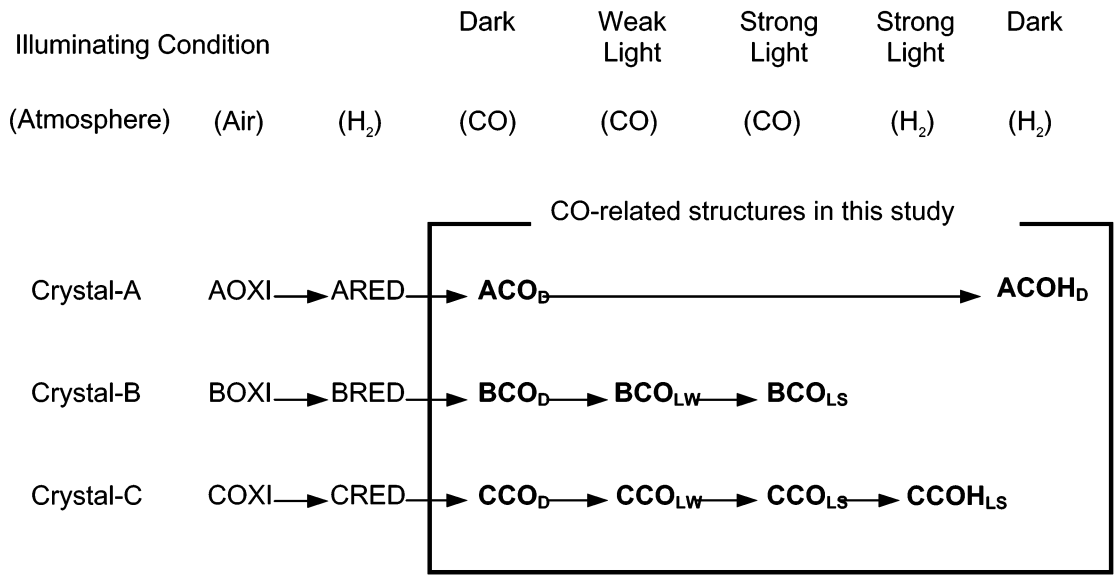

Figure 2. Diagrammatic explanation for the sample preparations for crystallographic studies of the CO-bound [NiFe]hydrogenase in three crystals. The oxidized forms for three crystals A, B, and C are shown as AOXI, BOXI, and COXI, whereas those in the H_2-reduced forms as ARED, BRED, and CRED, respectively. The CO-bound structures are represented as ACO, BCO, and CCO, and the illuminating condition is shown with a subscript of D (dark), LW (weak light), or LS (strong light). The nine CO-related structures analyzed in this study are enclosed by a box.

Table 1. Diffraction and Refinement Statistics of the Representative Structures among Three CO-Related Crystals

crystal	A	B		C
detector	R-AXIS	MAR-CCD		MAR-CCD
atmosphere	CO	CO	CO	CO
illuminating condition	dark	dark	light (strong)	dark
nomenclature	ACO_D	BCO_D	BCO_{LS}	CCO_D
space group: $P2_12_12_1$				
cell constants (Å)				
a	98.065	97.600	97.660	98.000
b	126.206	125.260	125.300	125.980
c	66.679	66.420	66.410	66.570
resolution (Å)	1.35	1.20	1.40	1.35
outer shell (Å)	1.42−1.35	1.25−1.20	1.48−1.40	1.41−1.35
completeness(%)	77.7	87.6	94.1	94.2
outer shell	47.6	68.1	81.8	93.4
R_{merge}	0.059	0.055	0.065	0.057
outer shell	0.299	0.339	0.658	0.352
R value ($>\sigma(F)$)	0.131	0.117	0.127	0.125
outer shell	0.218	0.194	0.261	0.205
R_{free} ($>\sigma(F)$)	0.178	0.151	0.189	0.162
reflections	139841	214464	114694	157769
parameters	59773	66023	59774	59965
reflections/parameters	2.3	3.2	1.9	2.6
water molecules	833	1070	836	967
2-methyl-2,4-pentanediol	11	7	5	0

collected separately. All diffraction experiments were carried out under a N_2 stream at 100 K. A summary of the data collection and processing statistics is shown in Table 1.

Nine structures in a series of CO-related [NiFe] hydrogenase using three crystals (Crystal-A, -B, and -C) from *D. v.* Miyazaki have been successfully determined, here the CO-related structures refer to the structures of the enzyme once exposed to CO, regardless of whether the CO was kept bound on the enzyme or removed by subsequent treatments. A sample preparation scheme is diagrammatically shown in Figure 2.

Each crystal grown in the oxidized form (AOXI; Crystal-A, BOXI; Crystal-B, and COXI; Crystal-C) under the normal air condition was reduced with H_2 (ARED, BRED, and CRED) and successively treated with CO in a glass capillary tube. Diffraction data sets of the CO-introduced structures were collected under dark conditions. Three CO-bound structures in their initial states after CO introduction in the dark are termed as ACO_D (A for crystal-A and the subscription D for the dark), BCO_D (crystal-B), and CCO_D (crystal-C). Crystal-A was incubated with H_2 for 1 h after data collection of ACO_D and was exposed to the X-ray beam in the dark ($ACOH_D$). After the data collection of BCO_D, the second data set was collected in the weakly lit ambient room light (BCO_{LW}, the subscription LW), followed by the third data set under a strong light at a distance of 50 mm from the crystal (BCO_{LS}, the subscription LS). Immediately after the data collection of CCO_{LS}, the CO gas was replaced with H_2 and the final diffraction data set of $CCOH_{LS}$ was collected under continuous illumination of a strong white light. Diffraction data images were indexed with the program DENZO[31] or MOSFLM,[32] and processed using SCALA in the CCP4 package.[33]

All nine structures have been refined at a resolution of 1.2−1.4 Å with R-values (free R-values) between 0.11 and 0.14 (0.15−0.19), using the program package CNS[34] followed by SHELXL.[35] During the SHELXL refinement, anisotropic temperature factors were introduced for the nonsolvent atoms in the protein molecule and the metal centers, except for the BCO_D structure, in which all the atoms were treated with anisotropic thermal motion. The nonprotein ligands, both the intrinsic diatomic ligands of the Fe atom in its native state and the exogenously added CO molecule, were refined without any stereochemical restraint in order to obtain the real features of the coordination geometry. The occupation factors of the exogenous CO ligand were refined at the final stage of the SHELXL refinement. The details of the refinement statistics of four out of nine structures are also listed in Table 1.

Spectroscopic Measurements. Optical absorption spectra of the [NiFe]hydrogenase in various states (oxidized, H_2-reduced, reoxidized, rereduced, and CO-added) were recorded at 288 K with a Shimadzu

(31) Otwinowski, Z.; Minor, W. *Methods Enzymol.* **1997**, *276*, 307−326.
(32) Leslie, A. G. W. MOSFILM, version 5.41; MRC Laboratory of Molecular Biology: Oxford University Press: Cambridge, UK, 1994.
(33) Collaborative Computational Project No 4. *Acta Crystallogr.* 1994, *D50*, 795−800.
(34) Brunger, A. T. *X-PLOR, version 3.1; A System for X-ray Crystallography and NMR*; Yale University Press: New Haven, CT, 1992.
(35) Sheldrick, G. M.; Schneider, T. R. Methods Enzymol. **1997**, *277*, 319−343.

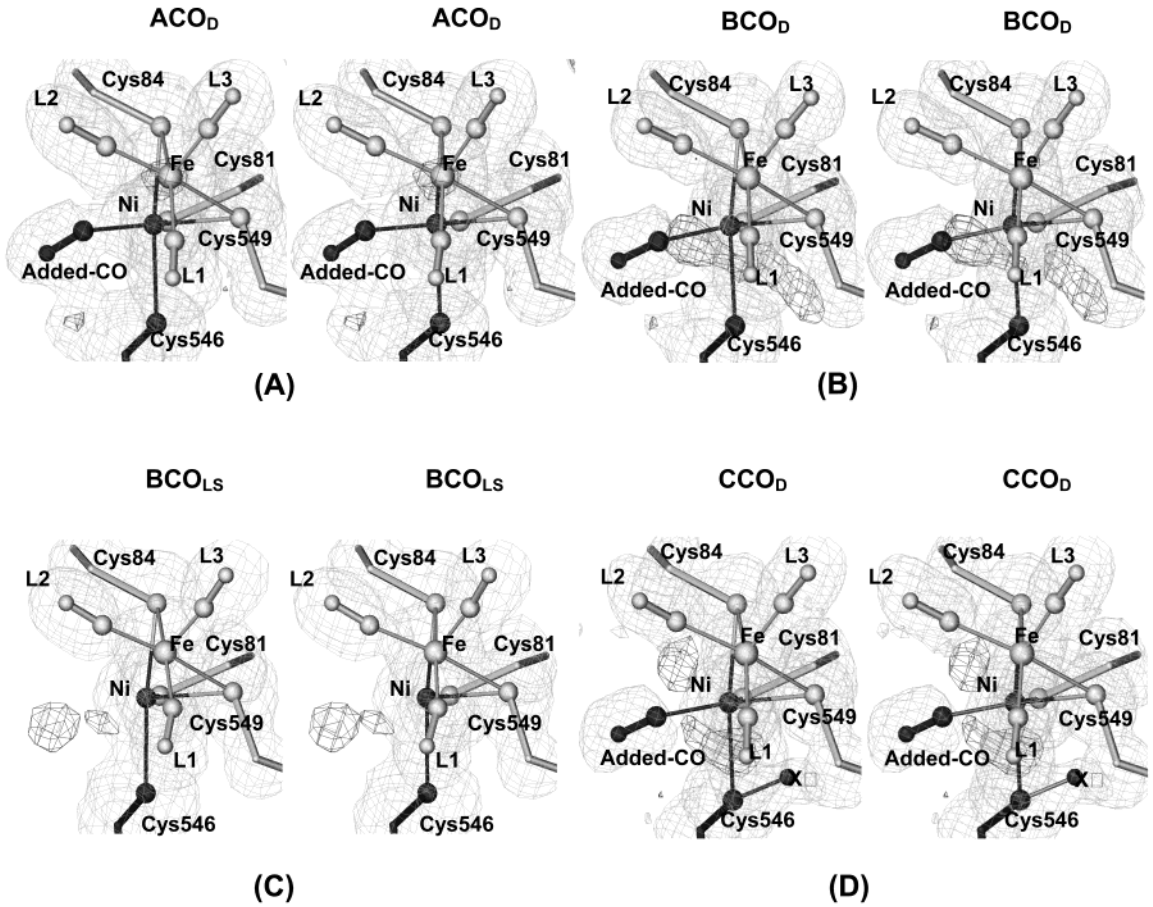

Figure 3. Omitted (3σ) and residual (4σ) Fo-Fc maps with a ball-and-stick model at the Ni−Fe active site. (A) Fo-Fc maps of ACO_D obtained under dark, (B) BCO_D under dark, (C) BCO_{LS} under illumination of a strong white light, and (D) CCO_D under dark. All structures were prepared under the CO atmosphere. The atoms shown in a ball-and-stick model were omitted in the calculation of the omit maps. Omit and residual maps are colored in gray and black, respectively. The Ni and Sγ (Cys546) atoms and the exogenous CO molecule are shown in black, whereas others in gray. All intrinsic diatomic ligands at L1, L2, and L3 sites are tentatively assigned as CO. Note that CO^I and CO^{II} ligands in our previous reports[8,13] correspond to L3 and L2, respectively. The figures were prepared using the program O.[37]

UV-3100PC spectrophotometer. Their difference spectra were calculated to eliminate the influence of the absorption of the protein moiety.

The resonance Raman scattering of the CO complex of [NiFe]-hydrogenase was excited at 476.5 nm with an Ar^+ ion laser (Spectra Physics, 2070) and detected at ambient temperature with a CCD (Princeton Instruments) attached to a triple polychromator (JASCO, NR-1800). The CO-bound [NiFe]hydrogenase was obtained by first reducing the oxidized hydrogenase with dithionite under H_2 atmosphere and then transferring the solution with a gastight syringe to the Raman cell filled with $^{12}C^{16}O$ or $^{13}C^{18}O$.

Results

Refined Structure. The overall folding pattern of the main-chain and the location of the metal centers were almost identical among all nine structures. The root-mean-square distances of the main-chain atoms calculated between any two structures in the same crystal were all within 0.12 Å, whereas those from different crystals were within 0.30 Å.[36] The size of the electron density of the L1 ligand, which was previously reported as SO in the oxidized and H_2-reduced forms,[8,13] was too small to assign an SO molecule in all the structures in this study. All Fe−CO angles appeared nearly linear after a few cycles of SHELXL refinement, and the coordination distances were between 1.7 and 2.0 Å. Consequently, it was difficult to specify the molecular species of the diatomic ligands based on the results in the highest-resolution structural analysis available at present. The Ni−Fe distance (2.61−2.62 Å) did not show any distinct changes on interaction of exogenous CO.

Binding Site for the Extrinsic CO. In the refined structure of the CO-bound [NiFe]hydrogenases (ACO_D, $ACOH_D$, BCO_D, BCO_{LW}, CCO_D, and CCO_{LW}), the added CO was found to coordinate to the Ni atom and not to the Fe atom at the Ni−Fe active site (Figures 3A, 3B, and 3D). The Ni−C distances of the extrinsic CO molecules were 1.76−1.78 Å, and the Ni−C−O were about 160° in BCO_D, BCO_{LW}, CCO_D, and CCO_{LW} structures. On the other hand, the CO-bound structures in Crystal-A showed a little different features (Ni−C = 1.72 Å and Ni−C−O = 135° for ACO_D). The occupation factor of the added CO was refined to 0.80 (ACO_D), 0.89 ($ACOH_D$), 0.96 (BCO_D), 0.91 (BCO_{LW}), 0.93 (CCO_D), and 0.83 (CCO_{LW}), respectively. The CO molecule, however, was hardly detectable in the initial $2F_O$-F_C maps of the BCO_{LS}, CCO_{LS}, and $CCOH_{LS}$ structures, and it was impossible to refine the atomic parameters of the C and O atoms of a CO during the refinement.

Unique Features of Electron Density Distributions at the Ni−Fe Active Site. There were several regions of isolated and/or connected electron density peaks larger than 3σ in the omitted

(36) During the refinement processes of all nine structures, it was realized that two assigned residues, Asp514-Val515, in the large subunit of [NiFe]-hydrogenase from *D. v.* Miyazaki are better described as Lys514−Leu515.

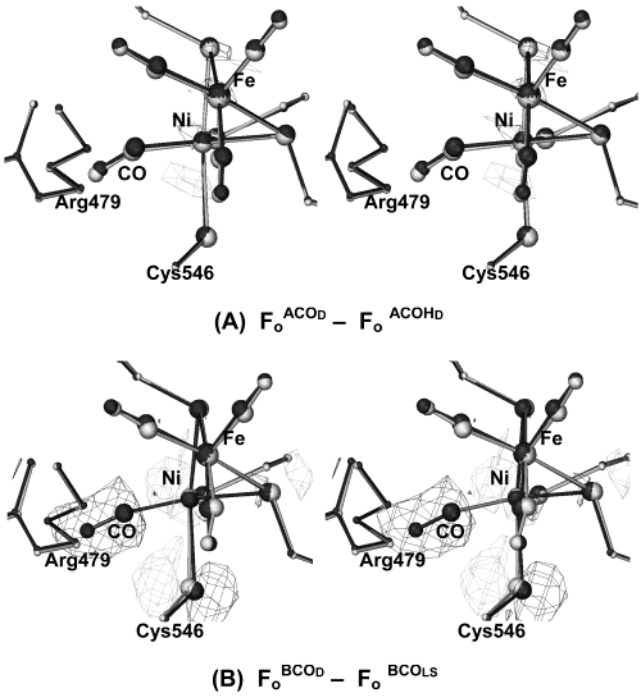

Figure 4. F_O-F_O difference Fourier maps with a ball-and-stick model of the active site calculated between two different structural states in each crystal: (A) F_O-F_O maps with the coefficients of $F_O^{ACO_D}-F_O^{ACOH_D}$ and α^{ACO_D} (black), and $F_O^{ACOH_D}-F_O^{ACO_D}$ and α^{ACOH_D} (gray), (B) $F_O^{BCO_D}-F_O^{BCO_{LS}}$ and α^{BCO_D} (black), and $F_O^{BCO_{LS}}-F_O^{BCO_D}$, and $\alpha^{BCO_{LS}}$ (gray). The figures were prepared using the program O.[37]

and 4σ in the residual F_O-F_C electron density maps around the Ni−Fe active site of the CO-related structures. One site was the exogenous CO site. All CO-liberated structures (BCO_{LS}, CCO_{LS}, and $CCOH_{LS}$) showed a small residual electron density peak at this site in both the omitted and residual electron density maps due to a trace of an exogenous CO (Figure 3C). As mentioned above, however, it was not possible to refine the atomic parameters of the fitted CO molecule at this site. The omitted and residual maps of the ACO_D and $ACOH_D$ structures showed one peak at the site between the exogenous CO and side-chain atoms ($C\beta$ and $S\gamma$) of Cys546 (Figure 3A), whereas the structures in Crystal-B and -C did not show any explicit electron density peak at this site in either the omitted or residual F_O-F_C maps except for CCO_{LW}. Instead, the electron density peaks of the $C\beta$ and $S\gamma$ atoms, however, extended toward the exogenous CO (Figure 3B). The BCO_D (Figure 3B), BCO_{LW}, BCO_{LS} (Figure 3C), CCO_D (Figure 3D), CCO_{LW}, and CCO_{LS} structures had another isolated peak at the site where the bridging sulfur ligand had been located in the oxidized form of the *D. v.* Miyazaki enzyme. The residual maps of the CCO_D (Figure 3D) and CCO_{LW} structures had an additional density peak between Cys81 and Cys84. The $ACOH_D$, BCO_D (Figure 3B), CCO_D (Figure 3D), CCO_{LW}, and CCO_{LS} structures had one more extra density peak near the $S\gamma$ atom of Cys546. This extra density was significant and located at a distance of covalent-bond length from $S\gamma$(Cys546) in both the omitted and residual maps in the CCO_D (marked X in Figure 3D), CCO_{LW}, and CCO_{LS} structures. This density peak disappeared on introducing H_2 under illumination of a strong white light in the structure of $CCOH_{LS}$. Except for this accompanying density peak, the structures of crystal C were essentially identical with those of crystal B. The origin and the nature of the accompanying peak will be dealt with elsewhere.

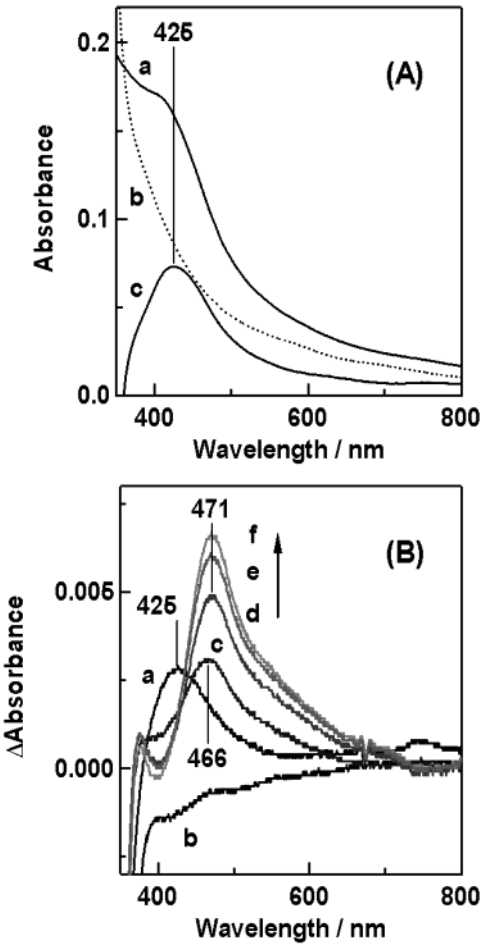

Figure 5. Absorption spectra of the [NiFe]hydrogenase from *D. v.* Miyazaki. (A) Absorption spectra of the (a) oxidized and (b) dithionite-reduced enzyme and (c) their difference spectrum. (B) Difference absorption spectra obtained by subtracting the spectrum of the reduced enzyme. (a) After incubation with a small amount of O_2 in the absence of H_2, (b) after H_2 re-incubation, and (c−f) after H_2 degassing and CO-re-incubation; (c) right after, (d) 30 min, (e) 1 h, and (f) 1.5 h after the introduction of CO. Concentration of the enzyme was 2.4 μM. Measured in 25 mM Tris-HCl buffer, pH 7.6, at 288 K.

In addition to the omitted and residual F_O-F_C maps, F_O-F_O maps were calculated between the data sets of two different states in the same crystal. All sets of F_O-F_O maps calculated between the CO-bound and CO-liberated forms exhibited a common feature; that is, there were two isolated electron density peaks (shown in black and gray) around the Ni and $S\gamma$(Cys546) atoms (Figure 4B: $F_O^{BCO_D}-F_O^{BCO_{LS}}$). In contrast, no distinct feature could be recognized in the maps between any two CO-bound (e.g. between the ACO_D and $ACOH_D$ structures shown in Figure 4A) or CO-liberated structures. On coordination of the exogenous CO to the Ni atom, $S\gamma$(Cys546) shifted away 0.2−0.3 Å from the original position. Other atoms comprising the Ni−Fe active site were also shifted to some extent, but only the electron density distributions of the Ni and $S\gamma$(Cys546) atoms were strongly affected. There was no distinct change in the electron density distribution around the Fe atom or its intrinsic diatomic ligands in any of the F_O-F_O maps.

Optical Absorption Spectra. Anaerobic incubation of purified [NiFe]hydrogenase with dithionite under H_2 atmosphere

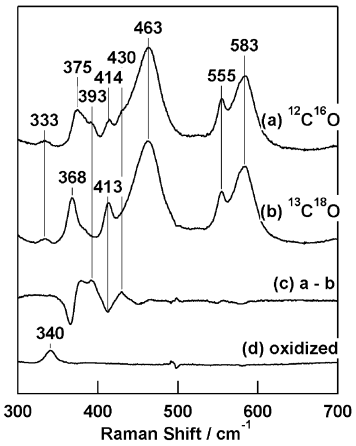

Figure 6. Resonance Raman spectra of the (a) $^{12}C^{16}O$ and (b) $^{13}C^{18}O$ complexes of the [NiFe]hydrogenase from *D. v.* Miyazaki, (c) their difference spectrum, and the spectrum of its oxidized form. Experimental conditions: excitation, 476.5 nm, 50 mW at the sample; sample, 80 μM enzyme in 25 mM Tris-HCl buffer, pH 7.6; ambient temperature.

resulted in a decrease in the intensity of the absorption band around 425 nm (Figure 5A), due to the reduction of the Fe−S clusters in the enzyme. The increase in the 470-nm band was time-dependent and saturated only after 6 h incubation under the CO atmosphere (Figure 5B). The absorption coefficient of the new band at 470 nm was estimated to be about 3000 $M^{-1}cm^{-1}$. A slight wavelength shift of the 470-nm band was concurrent with the decrease of the absorption around 425 nm, due to the gradual reduction of the remaining nonreduced enzyme by dithionite even after introducing CO. We attribute the new absorption band to the CO-bound complex of the reduced *D. v.* Miyazaki [NiFe]hydrogenase, because the wavelengths of the new absorption band was different from those of the oxidized Fe−S clusters, and the exogenous CO was shown to bind to the Ni atom in the crystal structures.

Resonance Raman Spectra. Several bands were detected in the resonance Raman spectra excited at 476.5 nm in resonance to the new absorption band (Figure 6, curves a and b), which had not been observed in the resonance Raman spectrum of the oxidized enzyme (Figure 6, curve d). Two CO-isotope-sensitive bands at 375 and 393 cm^{-1} were observed for the $^{12}C^{16}O$ complex due to Fermi resonance, which fused to one band at 368 cm^{-1} when $^{13}C^{18}O$ was used. Another band at 430 cm^{-1} for the $^{12}C^{16}O$-bound enzyme shifted to 413 cm^{-1} on incubation with $^{13}C^{18}O$. The shifts of these bands are clearly seen in the difference spectrum (Figure 6, curve c), while no significant frequency shift is observed in any of the other bands. Since the intensity of the Ni−C stretching (ν_{NiC}) band is expected to be higher than that of the Ni−C−O bending (δ_{NiCO}) band, the bands at 375/393 and 430 cm^{-1} are tentatively assigned to the ν_{NiC} and δ_{NiCO} Raman bands, respectively. The CO-isotope frequency shift for the ν_{NiC} band agreed with the value estimated by using the equation for a classical harmonic oscillator. The frequencies and their isotopic shifts in the resonance Raman spectra were also in parallel with those observed for nickel carbonyl: the ν_{NiC} band at 380 cm^{-1} of $Ni(CO)_4$ shifted to 376 cm^{-1} in $Ni(^{13}CO)_4$ and to 361 cm^{-1} in $Ni(C^{18}O)_4$, and the antisymmetric ν_{NiC} band (423 cm^{-1}) was observed at a lower frequency than the antisymmetric δ_{NiCO} band (455 cm^{-1}).[38]

Discussion

The overall structural features of the CO-bound and CO-liberated structures of the *D. v.* Miyazaki [NiFe]hydrogenase obtained from three crystals were essentially the same, confirming the reproducibility of the analyses, but some differences were recognized near the Ni−Fe site that is assumed to be the active site in the catalytic process to bind H_2. The results of the present work also reconfirmed the established structures reported in our earlier works[8,14] except in one point. The diatomic L1 ligand was refined to be a SO molecule in our previous works, [8,14] and a CO molecule in the present work. As L1 ligand is buried in the protein moiety and the structural features around the Fe atom with its ligands did not change during the CO-binding and CO-liberating cycles, it must be concluded that the crystals used in the present study had a CO (or CN) ligand at L1 site. The reasons of the discrepancy are not readily explainable, but one possibility is that the molecular species of the diatomic ligands of the Fe atom may be heterogeneous among the molecules. Heterogeneous features at the active site has been reported in the structural study of the [Fe]hydrogenase from *Clostridium pasteurianum*.[39]

Characteristics of the NiCO Site. Carbon monoxide, an inhibitor of the [NiFe]hydrogenase from *D. vulgaris* Miyazaki, was found to be bound to the Ni atom at the Ni−Fe site of the enzyme. Another case of CO binding to the Ni atom in a protein molecule has been reported for the Ni−Fe−S carbon monoxide dehydrogenase, [40] of which CO is a substrate rather than an inhibitor.

The $ACOH_D$ structure showed a CO-bound form, suggesting that most of the CO fractions in the Crystal-A remained at their coordination site in the dark at 100 K even in the H_2 atmosphere. The low temperature used for data collection might have hindered the CO liberation from the Ni atom, since CO association is known to be temperature-dependent. The occupation factors and the sizes of the electron density peaks of CO (BCO_D and CCO_D) diminished after illumination with a weak light (BCO_{LW} and CCO_{LW}). The exogenous CO ligand was almost liberated by illumination of a strong white light as shown in the BCO_{LS} and CCO_{LS} structures, leaving the intrinsic CO/CN ligands of the Fe atom in the Ni−Fe site unaffected (Table 2). These results suggest that illumination with a strong white light is more effective to remove the coordinated CO from the Ni atom than to replace CO with H_2 in the capillary tube at 100 K.

The Ni−C distances of the extrinsic CO molecules are about 1.77 Å except for the ACO_D structure (Table 2) and are similar to the typical coordination distances of CO binding to the Ni atom found in some Ni−CO complexes, e.g., the Ni−C distance of Ni(II) thiolate−CO complex being 1.75 Å.[41] However, the Ni−CO unit showed a bent conformation in all the CO-bound [NiFe]hydrogenase structures in this study. The range of Ni−C−O angles, 136.2 to 160.9°, seems to imply existence of

(37) Jones, T. A.; Zou, J. Y.; Cowan, S. W.; Kjeldgaard, M. *Acta Crystallogr.* **1991**, *A47*, 110−119.
(38) Jones, L. H.; McDowell, R. S.; Goldblatt, M. *J. Chem. Phys.* **1968**, *48*, 2663−2670.
(39) Peters, J. W.; Lanzilotta, W. N.; Lemon, B. J.; Seefeldt, L. C. *Science* **1998**, *282*, 1853−1858.
(40) Drennan, C. L.; Heo, J.; Sintchak, M. D.; Schreiter, E.; Ludden, P. W. *Proc. Nat. Acad. Sci. U.S.A.* **2001**, *98*, 11973−11978.
(41) Nguyen, D. H.; Hsu, H.-F.; Millar, M.; Koch, S. A. *J. Am. Chem. Soc.* **1996**, *118*, 8963−8964.

Table 2. Structural Parameters of the Ni−Fe Active Site of the Representative Four Structures

structure	ACO_D	BCO_D	BCO_{LS}	CCO_D
Ni−Fe distance (Å)	2.62	2.61	2.61	2.62
Extrinsic CO Ligands				
angle (deg) Ni−C−O	136.2	159.9		157.5
distance (Å)				
Ni−C	1.72	1.77		1.77
C−O	1.14	1.10		1.02
occupation factor	0.80	0.96		0.93
B (Å^2)				
C of CO	14.2	13.1		12.4
O of CO	16.4	17.5		12.7
Intrinsic CO Ligands[a]				
distance (Å)				
Fe−C(L1)	2.00	1.85	1.85	1.96
Fe −C(L2)	1.85	1.95	1.90	1.98
Fe−C(L3)	1.75	1.78	1.75	1.78
C−O(L1)	1.15	1.17	1.20	1.15
C−O(L2)	1.18	1.14	1.11	1.14
C−O(L3)	1.16	1.13	1.15	1.13
angle (deg)				
Fe−C−O(L1)	175.2	178.3	164.9	176.0
Fe−C−O(L2)	177.0	179.0	168.2	173.2
Fe−C−O(L3)	178.4	176.4	174.1	178.0
B (Å^2) of Sγ of Cys				
Cys81	12.5	11.1	13.9	10.3
Cys84	11.0	10.5	13.4	9.2
Cys546	15.7	14.6	20.1	12.6
Cys549	11.0	10.5	12.9	9.4

[a] Note that CO^I and CO^{II} in our previous reports[8,13] correspond to CO(L3) and CO(L2), respectively

several coordination modes (Table 2). The sizes and shapes of the electron density peaks are also different among the CO-bound structures. The coordination distances of the exogenous CO molecule to the Ni atom (1.77−1.78 Å) found in this high-resolution X-ray crystal structures were well in accordance with the value obtained by XAS experiment (1.78 Å).[27] However, the bent Ni−C−O structure was not in agreement with the results by XAS experiment.[27]

A new absorption band was detected at 470 nm for the CO-bound [NiFe]hydrogenase (Figure 5B), whereas the absorption of a CO complex of a Ni model compound ([PPN][Ni(CO)-$(SePh)_3$]) with λ_{max} at 419 (ϵ = 1979 $M^{-1}cm^{-1}$) has been reported previously.[42] Detection of exogenous CO-related Raman bands by excitation at 476.5 nm in resonance to the new CO-related absorption band strongly supported the assignment of the absorption band at about 470 nm to a CT band caused by coordination of the exogenous CO to the Ni atom.

In the Raman spectra, the bending mode would not appear if Ni−C−O was linear. The relatively high intensity of the δ_{NiCO} band as compared to the ν_{NiC} band should be due to the bent structure of the Ni−CO unit in solution as shown by the crystal structures.

The ν_{CO} frequency of the exogenous CO has been observed at 2060 cm^{-1} for the CO complex of [NiFe]hydrogenase from *C. vinosum*,[23] which was about 30 cm^{-1} higher than the ν_{CO} frequencies of Ni(I)− and Ni(II)−CO model compounds (2023−2029) cm^{-1}.[41,43,44] Similarly, the ν_{CO} band of the exogenous CO for the CO complex of [NiFe]hydrogenase from *D. fructosovorans* has been observed at 2055−2056 cm^{-1}.[45] The relatively high ν_{CO} frequency demonstrates a weaker π back-bonding from the filled d orbital of the Ni atom to CO in the CO complex of the [NiFe]hydrogenase, which is consistent with the relatively low ν_{NiC} frequency of the CO-bound [NiFe]-hydrogenase.

Activation Site for H_2. CO has been known to be a reversible and competitive inhibitor of [NiFe]hydrogenase. The facts that the exogenously added CO was coordinated to the Ni instead of the Fe atom and was liberated by a strong white light even at 100K in all CO-related structures imply that the substrate H_2 binds to the Ni atom (Figure 7). In addition, some novel structural features, which are described below, were found at the Ni−Fe active site in the series of the CO-related structures. These findings support the significant role of the Ni atom and the possible contribution of the Sγ(Cys546) atom for the catalytic reaction of the enzyme.

The most noteworthy characteristic is the distinct changes in the electron density distribution at the Ni and Sγ(Cys546) atoms between CO-bound and CO-liberated structures of all crystals, which were recognized in the Fo−Fo maps (Figures 4B). The changes suggest that the Ni and Sγ(Cys546) atoms are the most flexible sites during the CO-inhibition and reactivation processes of the enzyme. This is reasonable for the Ni atom, because the extrinsic CO molecule directly interacts with the Ni atom.

The second feature at the Ni−Fe active site is an additional electron density peak found between CO and Sγ(Cys546) in the ACO_D structure. The distance of 2.80 Å between the C atom of the CO and the Sγ(Cys546) atom in ACO_D was larger than the corresponding distances (2.5−2.7 Å) in other CO-bound structures. The existence of the significant electron density (larger than 4σ) might be indicative of the presence of some molecular species sandwiched or trapped between these atoms in ACO_D, which could be interpreted as the capture of an intermediate of the catalytic reaction.

In addition, the temperature factor of the Sγ(Cys546) atom was considerably larger than those of other liganding cysteine Sγ atoms in all structures, as well as for the oxidized and reduced structures reported previously.[8,13] The accompanying electron density peak found in Crystal-C and the distinguished high temperature factor of the Sγ(Cys546) atom strongly indicate that this is the most reactive site among all liganding sulfurs. The Sγ(Cys546) atom thus probably participates in the catalytic reaction at the active site. Another possible explanation for the high B-value of Sγ(Cys546) is that this sulfur atom may be hydrogenated, which would imply that the hydrogenation of the atom is essential for the catalytic reaction.[5,11,46−53] An additional interesting point is that the sulfur atom of Cys546 is replaced by a selenium atom in the [NiFeSe] hydrogenases found in some sulfate-reducing bacteria.[54−56]

(42) Liaw, W.-F.; Horng, Y.-C.; Ou, D.-S.; Ching, C.-Y.; Lee, G.-H.; Peng, S.-M. *J. Am. Chem. Soc.* **1997**, *119*, 9299−9300.
(43) Stavropoulos, P.; Muetterties, M. C.; Carrie, M.; Holm, R. H. *J. Am. Chem. Soc.* **1991**, *113*, 8485−8492.
(44) Marganian, C. A.; Vazir, H.; Baidya, N.; Olmstead, M. M.; Mascharak, P. K. *J. Am. Chem. Soc.* **1995**, *117*, 1584−1594.
(45) DeLacey, A. L.; Stadler, C.; Fernandez, V. M.; Hatchikian, E. C.; Fan, H.-J.; Li, S.; Hall, M. B. *J. Biol. Inorg. Chem.* **2002**, *7*, 318−326.
(46) Roberts, L. M.; Lindahl, P. A. *Biochemistry* **1994**, *33*, 14339−14350.
(47) De Lacey, A. L.; Hatchikian, E. C.; Volbeda, A.; Frey, M.; Fontecilla-Camps, J. C.; Fernandez, V. M. *J. Am. Chem. Soc.* **1997**, *119*, 7181−7189.
(48) Dole, F.; Fournel, A.; Magro, V.; Hatchikian, E. C.; Bertrand, P.; Guigliarelli, B. *Biochemistry* **1997**, *36*, 7847−7854.
(49) De Gioia, L.; Fantucci, P.; Guigliarelli, B.; Bertrand, P. *Inorg. Chem.* **1999**, *38*, 2658−2662.
(50) Niu, S.; Thomson, L. M.; Hall, M. B. *J. Am. Chem. Soc.* **1999**, *121*, 4000−4007.

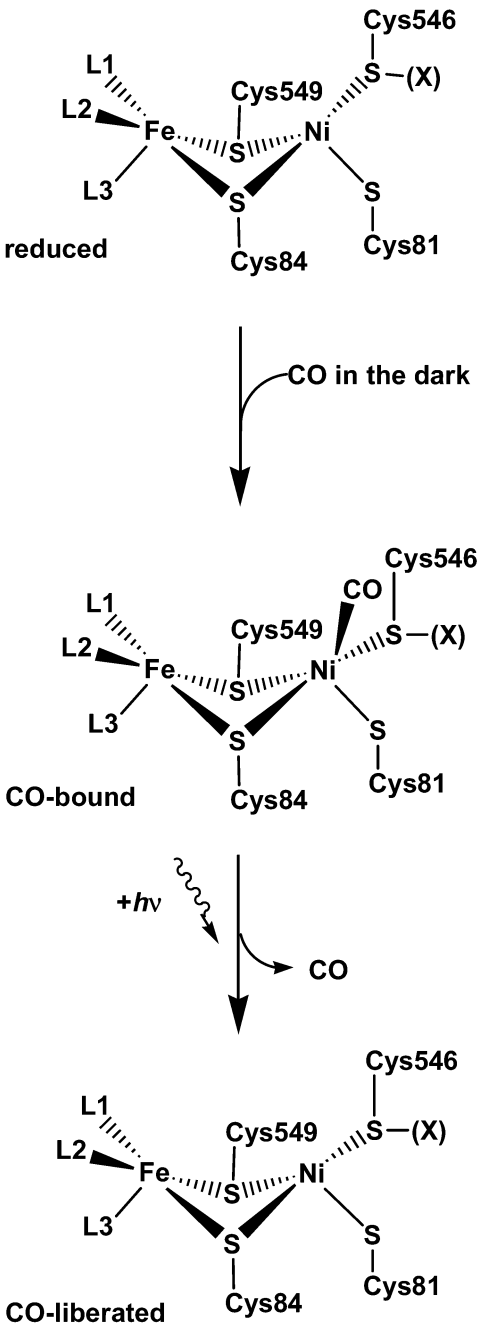

Figure 7. Schematic presentation of the Ni−Fe active site of the reduced, CO-bound, and CO-liberated forms of [NiFe] hydrogenase; L1 = SO, CN or CO; L2 = CN or CO; L3 = CN or CO.

Considering the structural features found in this study, we propose that the Ni and Sγ(Cys546) atoms play a role during the initial H_2 activation process at the Ni−Fe active site. The Fe atom and its accessory ligands are probably not involved in the initial activation process but could have a role in controlling the reaction by, for example, stabilizing the electronic states of the active site. In fact, the stereochemical parameters, the Ni−Fe distance, the coordination distances, and the angles of the intrinsic diatomic ligands (all tentatively assigned as CO) of Fe did not change significantly among all structures on interaction with the exogenous CO molecule (Table 2). However, this does not rule out a possibility that the Fe atom and its moiety are related with the successive catalytic reaction after the initial activation. Actually, the Ni−H^-−Fe intermediates are proposed after the heterolysis of a H_2.[11,13,47−52]

Conclusion

The exogenous CO was shown to coordinate to the Ni atom in a bent form by high-resolution X-ray crystal structure analysis. The Ni−C distances and Ni−C−O angles were about 1.77 Å and 160°, respectively, except for one case found in Crystal-A (1.72 Å and 135°). The coordinating CO molecule was not replaced with H_2 in the dark, but liberated by illumination of a strong white light at 100 K. The Fo−Fo maps calculated between the CO-bound and CO-liberated structures in each crystal showed a distinct change in the electron density distribution at the sites of Sγ(Cys546) and Ni, suggesting that they are the most flexible sites on interaction with exogenous CO. The coordination geometry of the intrinsic diatomic ligands of Fe or Ni−Fe distance did not show any distinct change on interaction with the exogenous CO. The CO-bound structure in Crystal-A showed an additional electron density peak between the CO and Sγ(Cys546). The temperature factor of the Sγ-(Cys546) atom was considerably larger than those of other liganding cysteine Sγ atoms in all structures, also implicating that it is the most reactive ligand and possibly the hydrogenation site during the catalytic reaction. The novel structural features found near the Ni and Sγ(Cys546) atoms in the series of the CO-related structures suggest that these two atoms at the Ni−Fe active site play a role during the initial H_2 activation process by the [NiFe]hydrogenase.

A new CT band at 470 nm was observed when CO was introduced to the reduced enzyme. The absorption coefficient of this new 470 nm band was estimated to be about 3000 $M^{-1}cm^{-1}$. Resonance Raman spectra of the CO-bound [NiFe]-hydrogenase exhibited a peak at 375/393 and 430 cm^{-1} for the $^{12}C^{16}O$ complex which shifted to 368 and 413 cm^{-1}, respectively, for the $^{13}C^{18}O$ complex. They are assigned to ν_{NiC} and δ_{NiCO} modes, respectively. The relatively high magnitude of the δ_{NiCO} band over the ν_{NiC} band suggested a significant bent structure for the Ni−CO unit, which is consistent with the crystallographic structure.

Acknowledgment. We are indebted to Professors Y. Igarashi and M. Ishii in The University of Tokyo, H. Akutsu at Osaka University, and Y. Shiro in RIKEN Harima Institute for their continuous support of our structural studies and helpful discussions. This work was supported in part by grants from the Ministry of Education, Culture, Sports, Science, and Technology of Japan (Nos. 12680654, 13014210, and 12740362), JBA, NEDO, and METI (a research grant for BREEZE and for Development of a Technological Infrastructure for Industrial Bioprocess on R&D of New Industrial Science and Technology Frontiers), the Toyota Physical and Chemical Research Institute, JAERI (a Reimei Research Grant), and the Japan Securities Scholarship Foundation.

JA012645K

(51) Pavlov, M.; Blomberg, M. R. A.; Siegbahn, P. E. M. *Int. J. Quantum Chem.* **1999**, *73*, 197−207.
(52) Amara, P.; Volbeda, A.; Fontecilla-Camp, J. C.; Field, M. J. *J. Am. Chem. Soc.* **1999**, *121*, 4468−4477.
(53) Maroney, M. J.; Bryngelson, P. A. *J. Biol. Inorg. Chem.* **2001**, *4*, 453−459.
(54) Menon, N. K.; Peck, H. D., Jr.; Gall, J. L.; Przybyla, A. E. *J. Bacteriol.* **1987**, *169*, 5401−5407.
(55) Pfeiffer, M.; Bingemann, R.; Klein, A. *Eur. J. Biochem.* **1998**, *256*, 447−452.
(56) Michel, R.; Massanz, C.; Kostka, S.; Richter, M.; Fiebig, K. *Eur. J. Biochem.* **1995**, *233*, 727−735.